THE JOURNAL OF PHYSICAL CHEMISTRY B

Article

pubs.acs.org/JPCB

How Strongly Does Trehalose Interact with Lysozyme in the Solid State? Insights from Molecular Dynamics Simulation and Inelastic Neutron Scattering

Adrien Lerbret,*[,†,⊥] Frédéric Affouard,[†] Alain Hédoux,[†] Stefanie Krenzlin,[‡,§] Jürgen Siepmann,[‡,§] Marie-Claire Bellissent-Funel,[∥] and Marc Descamps[†]

[†]Unité Matériaux Et Transformations, UMR CNRS 8207, Université Lille Nord de France, USTL, 59655 Villeneuve d'Ascq, France

[‡]University of Lille, College of Pharmacy, 3 rue du Professeur Laguesse, 59006 Lille, France

[§]INSERM U 1008, Controlled Drug Delivery Systems and Biomaterials, 3 rue du Professeur Laguesse, 59006 Lille, France

[∥]Laboratoire Léon Brillouin, UMR 12 CEA-CNRS, CEA-Saclay, 91191 Gif-sur-Yvette, France

Supporting Information

ABSTRACT: Therapeutic proteins are usually conserved in glassy matrixes composed of stabilizing excipients and a small amount of water, which both control their long-term stability, and thus their potential use in medical treatments. To shed some light on the protein−matrix interactions in such systems, we performed molecular dynamics (MD) simulations on matrixes of (i) the model globular protein lysozyme (L), (ii) the well-known bioprotectant trehalose (T), and (iii) the 1:1 (in weight) lysozyme/trehalose mixture (LT), at hydration levels h of 0.0, 0.075, and 0.15 (in g of water/g of protein or sugar). We also supplemented these simulations with complementary inelastic neutron scattering (INS) experiments on the L, T, and LT lyophilized (freeze-dried) samples. The densities and free volume distributions indicate that trehalose improves the molecular packing of the LT glass with respect to the L one. Accordingly, the low-frequency vibrational densities of states (VDOS) and the mean square displacements (MSDs) of lysozyme reveal that it is less flexible—and thus less likely to unfold—in the presence of trehalose. Furthermore, at low contents (h = 0.075), water systematically stiffens the vibrational motions of lysozyme and trehalose, whereas it increases their MSDs on the nanosecond (ns) time scale. This stems from the hydrogen bonds (HBs) that lysozyme and trehalose form with water, which, interestingly, are *stronger* than the ones they form with each other but which, nonetheless, relax faster on the ns time scale, given the larger mobility of water. Moreover, lysozyme interacts *preferentially* with water in the hydrated LT mixtures, and trehalose appears to slow down significantly the relaxation of lysozyme−water HBs. Overall, our results suggest that the stabilizing efficiency of trehalose arises from its ability to (i) increase the number of HBs formed by proteins in the dry state and (ii) make the HBs formed by water with proteins stable on long (>ns) time scales.

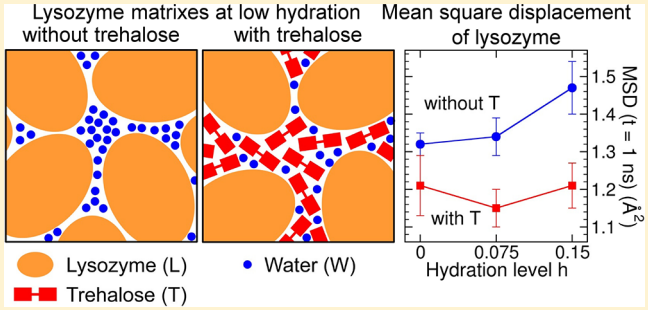

INTRODUCTION

Recent advances in molecular biology and recombinant technology have made a growing number of therapeutic proteins available for the treatment of cancers, diabetes, or brain diseases. However, these proteins are usually very labile in solution and are therefore conserved in solid amorphous matrixes, often prepared using lyophilization (freeze-drying).[1] Yet, this process induces severe temperature and/or dehydration stresses such as the formation of ice crystals, changes in pH and concentration, or phase separations, that may lead to the protein denaturation.[1] Thus, stabilizing solutes like sugars, polyols, polymers, and amino acids, which may act as *cryoprotectants* during freezing and/or as *lyoprotectants* during drying and storage, are often added to the liquid formulations.

The sources of physical and chemical degradations of proteins during their storage in lyophilized matrixes are numerous (aggregation, oxidation, browning, or Maillard reaction, etc.) and have focused considerable attention. The stability of proteins was shown to strongly depend on the composition (concentration of water, buffers, stabilizers, etc.) as well as on the storage conditions (temperature, humidity, etc.) of the freeze-dried matrixes.[1,2] It is now well established that an efficient stabilization of proteins in the solid state is achieved with both the formation of a glassy matrix (*vitrification* hypothesis[3]) and the intimate hydrogen bonding between

Received: June 13, 2012
Revised: August 14, 2012
Published: August 15, 2012

excipients and proteins (*water replacement* hypothesis[4]).[5−9] Vitrification actually slows down considerably protein conformational relaxations[10] and minimizes the rate of chemical reactions, while the substitution of protein hydration water by excipients satisfies the H-bonding requirements of protein surface polar groups, thereby preserving the native structure of proteins.[6,9,11] In comparison with other bioprotectants like polyols (glycerol, sorbitol, mannitol) and hydrophilic polymers (dextran, polyvinylpyrrolidone), the disaccharide trehalose (α-D-glucopyranosyl-α-D-glucopyranoside, $C_{12}H_{22}O_{11}$) represents a good trade-off between a high glass transition temperature and intimate H-bonding abilities with proteins. It is therefore commonly used for the long-term storage of proteins.[1,12] Trehalose is an osmolyte synthesized in small organisms (yeasts, larvae, tardigrades), called *anhydrobiotic*, that can withstand for very long periods of time severe environmental conditions of temperatures and/or dehydration.[4,5,9,12,13] Its physicochemical properties have been thoroughly investigated during the last two decades with the aim of deciphering the origin of its high protective efficiency.[12,14−18] Among many other properties, trehalose is characterized by (i) a high glass transition temperature T_g (∼393 K),[19] (ii) the absence of internal hydrogen bonds (HBs), which enhances its ability for intermolecular H-bonding with water and proteins, and (iii) a rich polymorphism,[15] and, in particular, a dihydrate crystalline phase, T_{2H_2O},[20] that may form in the amorphous matrix and, then, prevent its strong plasticization by water.[21]

Extensive work on proteins embedded in amorphous trehalose matrixes has provided valuable information on the protein−matrix coupling in the solid state.[22−34] Neutron scattering studies showed that the mean square displacements (MSDs) of myoglobin embedded in trehalose are similar to those of an amorphous trehalose matrix, thus suggesting that their motions are strongly coupled.[35] A tight protein−matrix coupling was also evidenced from the analysis of the temperature dependence of the CO stretching band of carboxy-myoglobin and that of the water association band of the related matrixes determined by Fourier transform infrared spectroscopy.[24] Similarly, Raman and neutron scattering studies indicated that both fast relaxations and low-frequency vibrations of lysozyme follow those of trehalose in the 100−350 K temperature range, therefore implying that trehalose controls protein's dynamics and activity.[25,26] Molecular dynamics (MD) simulations further evidenced a strong dynamical coupling between lysozyme and the surrounding amorphous trehalose matrix that arises from the protein−matrix HBs.[30] Moreover, carboxy-myoglobin embedded in a concentrated trehalose/water matrix was shown to be *preferentially* hydrated, sharing most of its hydration water with trehalose, whose presence significantly reduced the amplitude of the protein atomic mean square fluctuations compared to the protein in aqueous solution.[22,23] It was also inferred from infrared vibrational echo measurements that the trehalose glass inhibits large-scale atomic fluctuations of proteins and their hydration shell.[29] Water was found to form HB networks that anchor the protein surface to the embedding matrix, whose strength increases with a decrease of the water content (*anchorage hypothesis*).[28] Furthermore, the denaturation temperatures of several proteins (myoglobin, lysozyme, bovine serum albumin, and hemoglobin) embedded in trehalose/water matrixes were found to increase linearly with the glass transition temperature, T_g, of the protein/sugar/water matrix in recent differential scanning calorimetry (DSC) studies,[32,33] thus establishing a correlation between the unfolding of proteins and the structural relaxation of the matrixes. In addition, the degradation rates of enzymes such as lysozyme, horseradish peroxidase, and yeast alcohol dehydrogenase were found to decrease with the amplitude of fast, short-length scale motions of the protein/trehalose glasses,[27,34] which clearly evidence the importance of these motions for the stabilization of proteins in glassy matrixes.

To get further insight into the interactions between proteins, trehalose, and water in the solid state, we have compared three different amorphous matrixes: (i) lysozyme (L), (ii) trehalose (T), and (iii) the lysozyme/trehalose (LT) mixture (1/1 in weight) by means of MD simulations and inelastic neutron scattering (INS) experiments performed at 300 K. In the simulations, we have investigated the influence of water on the structural and dynamical properties of these matrixes at three hydration levels: h = 0.0, 0.075, and 0.15 in g of water/g of protein or sugar. This hydration range covers the typical water contents found in amorphous matrixes at the end of the lyophilization process and after exposure to moderate relative humidities,[1,7,36,37] and is well below those necessary to fully hydrate proteins (h ∼ 0.3−0.4).[38] We have studied the molecular packing in the matrixes from their *free volume* fractions and distributions. Moreover, we have determined the vibrational density of states (VDOS) and MSDs of lysozyme, trehalose, and water to characterize the coupling between their vibrational or diffusive motions. Finally, we have described intermolecular interactions in the simulated matrixes by the number, the geometry, and the dynamics of the different kinds of intermolecular HBs formed.

SIMULATION AND EXPERIMENTAL DETAILS

Molecular Dynamics Simulations. Molecular dynamics simulations have been performed using the CHARMM program.[39,40] The all-atom CHARMM22 force field[41] has been used to model hen egg-white lysozyme (hereafter referred to as lysozyme) using the CMAP correction for backbone dihedral angles.[42] The CHARMM carbohydrate force field[43,44] has been considered for trehalose, and water molecules were represented by the SPC/E model.[45] The length of all covalent bonds involving an hydrogen atom as well as the geometry of water molecules were kept fixed using the SHAKE algorithm,[46] with a relative tolerance of 10^{-10}. A 1 fs time step has been used to integrate the equations of motion with the Verlet leapfrog algorithm.[47] A cutoff radius of 10 Å has been employed to account for van der Waals interactions, which were smoothly force switched[48] to zero between 8 and 10 Å. Lorentz−Berthelot mixing rules have been considered for cross-interaction terms. Electrostatic interactions have been handled by the particle mesh Ewald (PME)[49] method with κ = 0.33 Å^{-1} and the fast-Fourier grid spacing set to ∼1 Å. During the different stages of the simulations, extended algorithms[50,51] were used to maintain system temperature and pressure. Most probable charge states at pH 7 were chosen for ionizable residues of lysozyme, whose total charge (+8 e) was then neutralized by uniformly rescaling the charge of protein atoms, as performed in previous simulations of lysozyme in aqueous solutions.[52−54] The initial conformation of trehalose molecules was that determined experimentally in the dihydrate crystal.[20]

The dry lysozyme (L) matrix consisted of eight lysozyme molecules in a tetragonal box with initial positions and orientations similar to those obtained from the X-ray crystal

structure of lysozyme solved at 1.33 Å (193L entry of the Brookhaven Protein Data Bank).[55] To generate the dry trehalose (T) glass, we inserted 334 trehalose molecules with random positions and orientations in a cubic simulation box with a 60 Å side length, corresponding to a density, ρ, of about 0.88 g·cm^{-3}. This rather low initial density prevented close interactions between sugars that may induce strong distortions of their rings during the subsequent minimization procedure. The lysozyme/trehalose (LT) mixture was composed of 8 lysozyme and 334 trehalose molecules inserted with random positions and orientations in a cubic simulation box with an initial side length of 76 Å ($\rho \sim 0.87$ g·cm^{-3}). We generated each hydrated system from the dry glasses, by inserting water molecules with random positions and orientations. Initial configurations were minimized with the steepest descent and conjugate gradient algorithms, heated up from 100 to 300 K at a rate of 5 K/ps, and equilibrated for 100 ps in the canonical ensemble. Then, we performed two successive simulations in the isobaric−isothermal ensemble for 1 ns at a pressure of 1 and 2000 atm, respectively. The second simulation aimed at densifying the simulation boxes initially generated at rather low densities (see above) without denaturing lysozyme molecules and/or changing significantly the conformations of trehalose molecules. The configuration obtained was relaxed by performing a simulation of 200 ps at 1 atm. Following this preequilibration procedure, each system was heated up from 300 to 700 K at a rate of 0.5 K/ps, equilibrated at 700 K for 3 ns, and then cooled down to 300 K at a rate of 0.05 K/ps. During this part of the equilibration procedure, we constrained lysozyme molecules with a mass-weighted bestfit harmonic potential of 1.0 kcal/mol/Å^2 to prevent any significant protein conformational changes. Next, we performed an additional equilibration at 300 K for 3 ns to check for volume stabilization. The densities of the dry trehalose and lysozyme glasses obtained using this procedure are smaller by about 5% than those available in the literature. Previous simulation studies[56−58] indeed reported densities of 1.45−1.47 g/cm^3 for the trehalose glass at 300 K, and values of about 1.50−1.53 g/cm^3 were obtained experimentally for lyophilized trehalose.[59−61] Similarly, densities of 1.237 and 1.363 g/cm^3 were determined for the dry lysozyme crystal in refs 62 and 63, respectively. These slight differences, ascribed to the various preparation protocols and force fields employed, are not expected to change the general trends of the results reported in this study. Finally, we run simulations at 300 K in the canonical ensemble for 25 ns at the equilibrated volume and saved configurations every 0.2 ps for analysis. Table 1 summarizes some simulation data for the different systems considered in the present study. Furthermore, the average contents of secondary structure (α-helices and β-sheets) of lysozyme in the L and LT mixtures are given in Table S1 in the Supporting Information. They show that the conformation of lysozyme remains similar to its native one[55] in the L and LT glasses.

Preparation of Freeze-Dried Samples. Lysozyme from chicken egg white (lyophilized powder) and trehalose dihydrate were purchased from Sigma Aldrich (Lyon, France). Lysozyme powder and trehalose dihydrate were accurately weighted and dissolved in Milli-Q water so as to give 500 mL solutions at concentrations of 5% (w/v). Additionally, 500 mL of a 5% (w/v) solution at a 1:1 mass ratio of lysozyme powder and trehalose dihydrate was prepared. The required amount of the disaccharide was calculated on the basis of the trehalose anhydrate. Freeze-drying was conducted in a shelf freeze-dryer (Epsilon 2-4 LSC; Martin Christ Gefriertrocknungsanlagen; Osterode, Germany). The protein and trehalose solutions were frozen to 228 K at 1 K/min and equilibrated for 1 h. Primary drying was conducted at 264 K at a vacuum of 0.014 mbar for 10 h, followed by secondary drying (T = 293 K, P = 0.0014 mbar) for an additional 10 h. Freeze-dried powders were stored in sealed containers at 277 K.

Table 1. Compositions and Densities of the Different Simulated Matrixes (Where N_L, N_T, and N_W Denote the Number of Lysozyme, Trehalose, and Water Molecules, Respectively) as a Function of the Hydration Level h, Which Refers to the Weight Fraction of Water with Respect to Either Lysozyme in the L and LT Glasses or Trehalose in the T Glass

system	h (g of H_2O/g of L or T)	N_L	N_T	N_W	ρ (g·cm^{-3})
L	0.0	8	0	0	1.179
	0.075	8	0	477	1.217
	0.15	8	0	954	1.228
LT	0.0	8	334	0	1.288
	0.075	8	334	477	1.307
	0.15	8	334	954	1.307
T	0.0	0	334	0	1.390
	0.075	0	334	477	1.397
	0.15	0	334	954	1.377

Neutron Scattering Experiments. Inelastic neutron scattering (INS) experiments were performed on the Mibémol time-of-flight (TOF) spectrometer of the Orphée reactor at Laboratoire Léon Brillouin (LLB) in Saclay, France. Aluminum flat rectangular cells with a thickness of 0.4 mm were used. Measurements were carried out at 300 ± 1 K with a wavelength of 6.0 Å and an energy resolution of about 100 μeV (full width at half-maximum, fwhm). The spectra of the lyophilized lysozyme, trehalose, and lysozyme/trehalose samples as well as that of the empty cell were recorded for about 12 h. Standard corrections of the raw data (normalization by monitor count, vanadium normalization to correct for detector efficiency and empty cell subtraction) were performed using the QENSH program.

The vibrational density of states (VDOS) was determined from the vibrational incoherent dynamic structure factor $S^{vib}_{inc}(Q,\omega)$ as follows:

$$G(\omega) = \sum_Q \frac{\omega \cdot S_{inc}(Q,\omega)}{n(\omega)\cdot Q^2(\omega)} \quad (1)$$

where $n(\omega)$ is the Bose population factor.

In the simulations, we calculated the low-frequency VDOS from the Fourier transform of the mass-weighted autocorrelation function of atomic velocities:

$$c_{vv}(t) = \frac{1}{M}\sum_{i=1}^{N} m_i \langle \mathbf{v}_i(0)\cdot\mathbf{v}_i(t)\rangle \quad (2)$$

where $\mathbf{v}_i$ is the velocity vector of atom i and m_i its mass and $M = \sum_i m_i$ is the mass of all the atoms considered in the calculation. The VDOS is then written as

$$g_{vv}(\omega) = \int_0^\infty \cos(\omega t) c_{vv}(t)\, dt \quad (3)$$

The average VDOS have been computed from 25 10 ps simulations, for which atomic coordinates and velocities have been recorded every 2 fs, and whose starting points were taken

dx.doi.org/10.1021/jp3058096 | J. Phys. Chem. B 2012, 116, 11103−11116

every ns from the production simulations described above. Averaging over these relatively short simulations yielded standard deviations on the computed VDOS that were small enough to ensure that the reported trends were statistically meaningful.

Furthermore, we determined the mean square displacement, $\langle r^2 \rangle$, of the hydrogen atoms in the lyophilized L, LT, and T matrixes from the elastic incoherent scattering intensity, $S_{inc}(Q,\omega = 0)$, using the Gaussian approximation:[64]

$$\langle r^2 \rangle = -6 \cdot \frac{d(\ln[S_{inc}(Q, \omega = 0)])}{d(Q^2)}\Bigg|_{Q=0} \quad (4)$$

where $\langle r^2 \rangle = \langle |\mathbf{r}(t) - \mathbf{r}(0)|^2 \rangle$ is the average mean square displacement on the time scale of the instrumental resolution, Δt (Δt [ps] $\approx$ 2*0.658/fwhm [meV] $\approx$ 13.2 ps).

RESULTS

Densities - Free Volume. We have first determined the densities, ρ, of the simulated systems to roughly compare their molecular packing (Figure 1a and Table 1). At a given hydration level h, ρ steeply increases with the trehalose content. Indeed, the much smaller size of trehalose with respect to lysozyme (radii of gyration of about 3.5 and 14.3 Å, respectively) gives rise to much smaller *excluded volume effects*, which are responsible for the poor packing efficiency of protein molecules. Such a trend has been observed recently on the IgG1 protein lyophilized with or without sucrose,[65] and it is well in line with the larger density of lyophilized trehalose[59−61] compared to that of lyophilized proteins.[61] Adding a small amount of water (h = 0.075) induces a significant increase of the density of the L and LT glasses, therefore suggesting that water is filling the available free volume (holes) found in the anhydrous glasses (Figure 2). This behavior is fully consistent with the reduction of hole volume in glassy maltopolymer−maltose and maltodextrin−glycerol matrixes observed by means of positron annihilation lifetime spectroscopy (PALS) upon sorption of water up to weight fractions of ~0.04−0.08.[66,67] In contrast, the density increase is very slight for the much more dense T glass, and it may be partially accounted for by the rather low packing density of trehalose molecules with the CHARMM force field. Indeed, using another force field that leads to a higher density for the trehalose glass, Simperler et al. found the density of trehalose/water mixtures to decrease when the hydration level h increases from 0.0 to 0.053.[68] Furthermore, while the density of the L glass keeps increasing when h raises from 0.075 to 0.15, that of the T glass decreases, in agreement with the well-known *plasticizing* effect of water on carbohydrate matrixes.[69,70] Interestingly, the density increase observed upon addition of water is opposite to the decrease expected assuming an ideal mixing behavior of the components (lysozyme, trehalose, and water), which occupy an average molecular volume of about 20 200, 410, and 30 Å^3, respectively, in the simulated bulk systems. Therefore, Figure 1a suggests nonmonotonic dependencies of ρ with the water content h (i.e., a first increase at low values, and then a decrease at larger

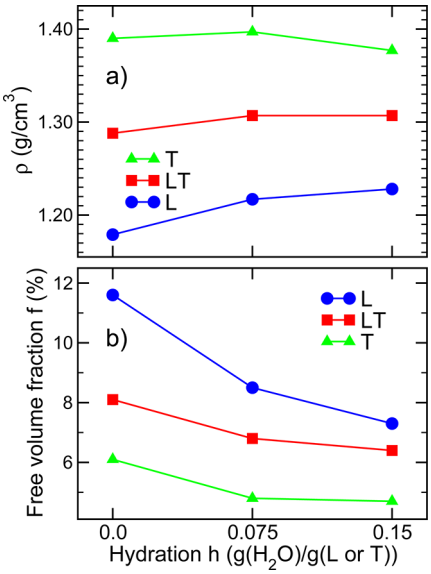

Figure 1. (a) Density, ρ, and (b) free volume fraction, f, of the lysozyme (L), lysozyme/trehalose (LT), and trehalose (T) matrixes as a function of the hydration level h. f denotes the ratio of the total free volume accessible to a probe radius of 0.5 Å, V_f, to the total volume of the simulation box V (f = 100*V_f/V). Standard deviations from mean values are smaller than the size of symbols and are thus not shown.

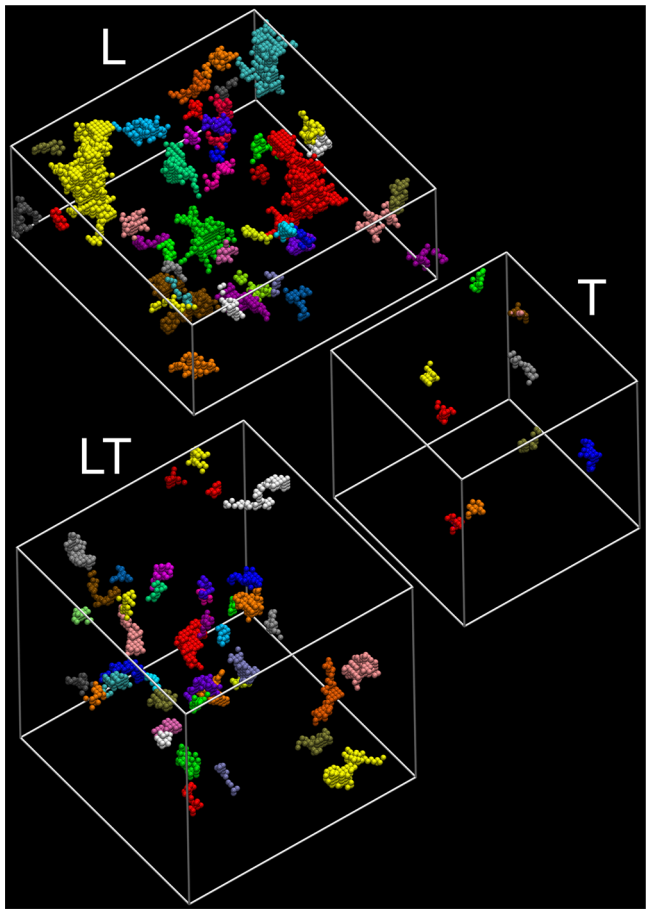

Figure 2. Free volume spatial distributions in representative configurations of the anhydrous lysozyme (L), lysozyme/trehalose (LT), and trehalose (T) glasses, accessible to a probe radius of 1.0 Å. For clarity, holes are colored in various colors, and only the holes whose volume is larger than about 15 Å^3 are displayed. The simulation boxes are represented by the white lines. The dimensions of the tetragonal box of the L glass are about 7.2*7.2*3.2 nm^3, and the side lengths of the cubic boxes of the LT and T systems are close to 6.7 and 5.2 nm, respectively. This figure was generated using VMD[73] (http://www.ks.uiuc.edu/Research/vmd/).

dx.doi.org/10.1021/jp3058096 | J. Phys. Chem. B 2012, 116, 11103−11116

values), which imply a peculiar role of water on the molecular packing properties of the studied glasses.

To gain further insight into this role, we have computed their free volume fraction, f,[71] in a similar way as in ref 72. The free volume fraction f represents the ratio of the total free volume accessible to a probe of radius r, V_f, to the total volume of the simulation box, V ($f = 100*V_f/V$).[71] The free volume fractions f computed with a probe radius of 0.5 Å are shown in Figure 1b. They decrease significantly upon addition of a small amount of water, clearly showing that water molecules are filling the small voids found in the anhydrous glasses. This result is in line with those obtained in a previous MD simulation study of sucrose matrixes at various water contents (0−50 wt %), where f was found to decrease from ∼5% for anhydrous sucrose down to ∼3.5% upon addition of 10 wt % water.[72] Moreover, the much larger f value for the L glass with respect to that for the T one is consistent with previous estimations of f in protein/sucrose glasses using gas pycnometry, which indicated that f decreases monotonically with the sucrose weight content: from 15% in the dried therapeutic protein matrix (0 wt % sucrose) down to 3% in amorphous sucrose, given the tighter packing of sucrose molecules.[65] Accordingly, f is found smaller in the LT mixture than in the L glass, owing to the presence of trehalose, which intercalates between lysozyme molecules, thus improving the molecular packing.

We have then characterized the spatial and size distributions of holes in the systems, because they provide a more detailed picture of the molecular packing than f, which only gives the average amount of the free volume available. Those of the anhydrous L, LT, and T glasses are shown in Figures 2 and in 3a, respectively. Striking differences are observed: whereas only small and isolated voids exist in the anhydrous T system, large and almost percolating holes are found in the L glass. In particular, two large holes (colored in yellow and red in Figure 2) clearly reveal the significant excluded volume effects arising from the large size and the nonoptimal packing of lysozymes.

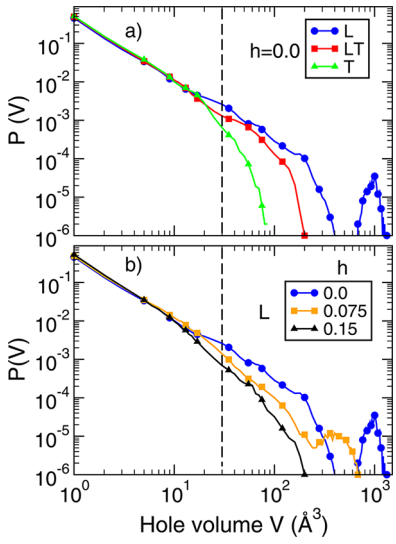

Figure 3. Probability distribution functions of the size of free volume holes accessible to a probe radius of 1.0 Å, $P(V)$: (a) in the anhydrous lysozyme (L), lysozyme/trehalose (LT), and trehalose (T) glasses and (b) in the L matrixes as a function of the hydration level h. The vertical dashed lines appearing at V = 30 Å^3 represent the average volume occupied by water molecules in the bulk in room conditions (ρ = 1.0 g·cm^{-3}).

These two large holes contribute to the peak close to 1000 Å^3 observed in the free volume distributions of the dry L matrix in Figure 3. Figure 3a also indicates that many of the molecular voids are large enough to be filled by water molecules, which explains the strong density increase observed in Figure 1a. In the presence of trehalose, the number of holes of size greater than ∼200 Å^3 strongly decreases in the LT glass, which is likely to limit the existence of large clusters of water such as those found in the hydrated L glass (see Figures S1 and S2 in the Supporting Information). As expected, the probability of finding large holes in the anhydrous T glass is very small, given the higher molecular packing efficiency of trehalose compared to lysozyme. Figure 3b explicitly shows the progressive disappearance of large holes in the L matrixes upon addition of water, which supports the filling of large holes by water molecules proposed above. Note, however, that this filling remains partial in the L matrix at h = 0.075, as indicated by the peak close to 450 Å^3 in the corresponding distribution shown in Figure 3b. Therefore, large holes (>200 Å^3) do not vanish at this hydration level and are thus likely to exist in lyophilized protein samples, owing to the usual hydration levels found in those matrixes (h < 0.05−0.1).[1,7,36,37]

In Figure 4, we summarize the results from Figures 1, 2, and 3 as a schematic representation of the L and LT systems, which

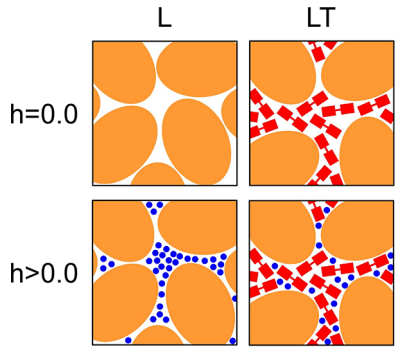

Figure 4. Schematic representation of the L and LT matrixes in the absence (top panel) and in the presence (bottom panel) of a small amount of water. Lysozyme, trehalose, and water molecules are shown as orange-filled ellipses, red interconnected rectangles, and blue disks, respectively.

will facilitate the interpretation of the results on the protein−matrix intermolecular interactions described below. The large size and globular shape of lysozyme make the existence of big holes ineluctable in the dry L glass, owing to strong excluded volume effects. Adding a small amount of water progressively fills these holes, leading to an increase of the density and a decrease of the available free volume, as well as to the formation of clusters of water molecules (see Figures S1 and S2 in the Supporting Information). Moreover, the picture of the LT system suggests that (i) trehalose limits protein−protein contacts, (ii) the presence of lysozyme is likely to disorganize the packing of trehalose molecules, (iii) water molecules can bridge the protein surface to the surrounding matrix, and thus improve the protein−matrix coupling, and (iv) water−water interactions are reduced in the hydrated LT matrix, which is likely to limit water mobility. In the following, we will analyze and discuss all of these points.

Vibrational Densities of States. The low-frequency part of the vibrational density of states (VDOS), $g(\omega)$, of proteins is very sensitive to their environment. For instance, an increase in

dx.doi.org/10.1021/jp3058096 | J. Phys. Chem. B 2012, 116, 11103−11116

the low-frequency (ω < 20−30 cm^{-1}) $g(\omega)$ of the enzyme dihydrofolate reductase (DHFR) has been observed upon binding of the methotrexate (MTX) ligand, thereby indicating the protein softening.[74,75] Furthermore, the low-frequency part (ω < 50 cm^{-1}) of the $g(\omega)$ of lysozyme was found to be shifted to higher frequencies upon addition of 37−60 wt % of the trehalose, sucrose, and maltose disaccharides to the aqueous solution, which evidences a stiffening of the protein motions.[76] Thus, the VDOS can provide useful information on the coupling of vibrational motions in the studied glasses. In Figure 5, we compare the VDOS of the L, LT, and T glasses at h = 0.075 with those of the lyophilized lysozyme, lysozyme/trehalose, and trehalose samples deduced from INS experiments. The simulated $g(\omega)$ are slightly shifted to lower frequencies in comparison with the experimental ones, thus indicating softer intermolecular interactions. This feature has been observed previously by Balog et al.[77] for the DHFR enzyme, and may arise from the limited accuracy of the force fields used and from the different local structures, homogeneities, and densities of the simulated systems. However, the relative distributions of modes of the three simulated mixtures are in fair agreement with those obtained from neutron scattering, which indicates that intermolecular interactions are satisfactorily reproduced in the simulations. The broad peak centered near 60−80 cm^{-1} has been assigned to the harmonic vibrations that atoms experience within the *cage* formed by their neighbors,[78] by analogy with the band found around 50−60 cm^{-1} in liquids.[79,80] It is found broader in the L glass, given the greater heterogeneity of the environments experienced by protein residues with respect to trehalose and water molecules. Interestingly, the number of very low-frequency modes (ω < 30 cm^{-1}) decreases with the protein concentration. This implies that protein residues experience more anharmonic and larger-scale motions than trehalose molecules. Furthermore, the VDOS intensity in this frequency range decreases with an increase of the density of the simulated systems, suggesting that the more dense packing in the trehalose glass hinders to a greater extent large-scale intermolecular motions. Besides, it is not straightforward to analyze intermolecular interactions between lysozyme, trehalose, and water from the spectra shown in Figure 5, given the superimposition of the contribution of each species. Thus, we have determined from the MD simulations the VDOS of individual species, some of which are displayed in Figure 6.

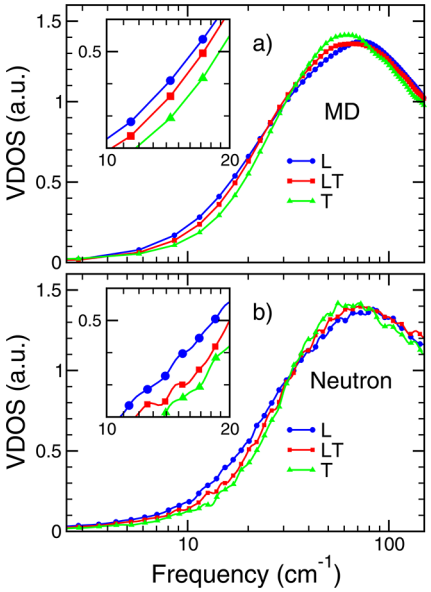

Figure 5. Vibrational densities of states (VDOS), $g(\omega)$, (a) of the simulated L, LT, and T glasses at h = 0.075 and (b) of the lyophilized lysozyme, lysozyme/trehalose, and trehalose samples obtained experimentally by inelastic neutron scattering. Each spectrum was normalized in the 0−100 cm^{-1} range for comparison purposes. To make the comparison easier, a larger view of the 10−20 cm^{-1} region is shown in the inset of each figure. Moreover, experimental curves were smoothed with the Savitzky−Golay algorithm.[81]

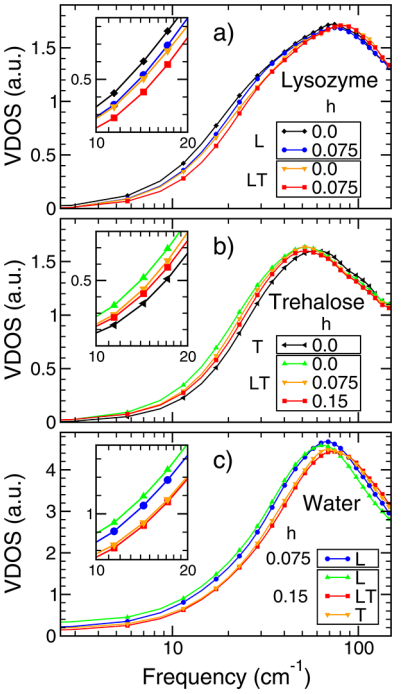

Figure 6. Vibrational densities of states (VDOS), $g(\omega)$, of (a) lysozyme, (b) trehalose, and (c) water in various matrixes. The insets magnify the 10−20 cm^{-1} frequency range to make the comparison between the different systems easier.

At a given hydration level, the low-frequency part (<50 cm^{-1}) of the VDOS of lysozyme in the LT glass is shifted to higher frequencies in comparison with the L glass (Figure 6a), therefore suggesting that the environments experienced by the residues of lysozyme are more rigid in the presence of trehalose. This is consistent with the low-frequency Raman spectra obtained by Caliskan et al.,[25] in which the position of the *boson* peak was found at a higher frequency in the lysozyme/trehalose glass than in the dry lysozyme one. A similar high-frequency shift has also been observed on lysozyme upon addition of disaccharides to the aqueous solution.[76] In contrast, the low-frequency range of the VDOS of trehalose is shifted to lower frequencies in the LT glasses in comparison with the T glasses (Figure 6b), thereby implying a looser packing of trehaloses in the LT mixtures, in agreement with the free volume analysis performed above. These results show that the strength of the *cage* effect experienced by molecules is very sensitive to their local packing, and thus to the local free volume available. The addition of water to the L and LT glasses induces a high-frequency shift of the VDOS of both lysozyme and trehalose (Figure 6a,b), in line with the corresponding increases in density observed in Figure 1a. Besides, the low-frequency

dx.doi.org/10.1021/jp3058096 | J. Phys. Chem. B 2012, 116, 11103−11116

VDOS of water in the different systems (Figure 6c) are significantly high-frequency shifted with respect to that of liquid bulk water (see Figure 1 in ref 82), which implies that the environments experienced by water molecules are much stiffer in the considered systems. This behavior is comparable to that obtained for water in disaccharide[82] and lysozyme/disaccharide[76] aqueous solutions, as well as in the hydration shell of proteins such as the HP36 villin headpiece subdomain[83] or the λ^*_{6-85}-repressor.[84] It was shown to be correlated with a significant slowing down of the dynamics of water HBs[82,84] and to be more important for hydrophobic residues owing to sterical effects.[84] Furthermore, the high-frequency shift is smaller in the L systems than in the LT and T ones, as could be expected from the absence of trehalose with which water interacts strongly via HBs (see sections on HBs). This high-frequency shift also weakens with an increase of the hydration level from 0.075 to 0.15, given that the probability of water−water interactions, which reduce the constraints imposed on water molecules, increases with h.

Mean Square Displacements. We determined the mean square displacements (MSDs), $\langle r^2 \rangle$, of the lyophilized L, LT, and T matrixes from the incoherent neutron scattering spectra using eq 4 and found values of 0.74 ± 0.05, 0.59 ± 0.04, and 0.42 ± 0.06 Å^2, respectively. These MSDs essentially represent the motions of hydrogens on a time scale of about 13.2 ps, owing to the instrumental energy resolution used for the measurements (fwhm ≈ 100 μeV). For comparison, the MSDs of the simulated L, LT, and T matrixes at h = 0.075 and time t = 13.2 ps are 0.85 ± 0.02, 0.61 ± 0.01, and 0.59 ± 0.01 Å^2, that is, in reasonable agreement with the neutron scattering data. Note that the larger difference between the experimental and numerical MSDs for the T system may stem in part from a larger difference between the densities of the freeze-dried and simulated T glasses (see section Molecular Dynamics Simulations). The lower MSD of the T matrix compared to that of the L one is in accordance with the smaller number of low-frequency vibrational modes and with the higher density of the T matrix (see Figures 5 and 1, respectively). This result corroborates those of Wang et al.,[65] who found that the mean square displacement of sucrose at the nanosecond time scale is smaller than that of the protein cytokine. Similarly, Cicerone and Douglas showed that the MSDs of freeze-dried protein/sugar glasses composed of sucrose and either lysozyme, cytokine, or immunoglobulin G (IgG) decrease with the sugar mass fraction.[34] Accordingly, the MSD of the LT matrix is found intermediate between those of the L and T matrixes. Then, we have computed the MSDs of lysozyme and trehalose at shorter (t = 1 ps) and longer (t = 1 ns) time scales from the MD simulations to further probe the effect of water and trehalose on both the fast and the *slow* dynamics of lysozyme (see Figure 7a and b, respectively). For clarity, the corresponding MSDs of water are given separately in Table 2. Whatever the time scale considered, lysozyme obviously experiences stiffer environments in the presence of trehalose. This agrees with the above results on the vibrational densities of states (see Figure 6a) and with the significant reduction of the mean square fluctuations of the backbone atoms (C, C$_\alpha$, N) of lysozyme in aqueous solution upon addition of trehalose at 37−60 wt % concentrations.[53] It indicates that at the considered protein/sugar ratio (1:1 in weight) trehalose both limits the amplitude of protein fast motions as well as slow protein conformational relaxations. Interestingly, the effect of water on the MSD of lysozyme strongly depends on the time

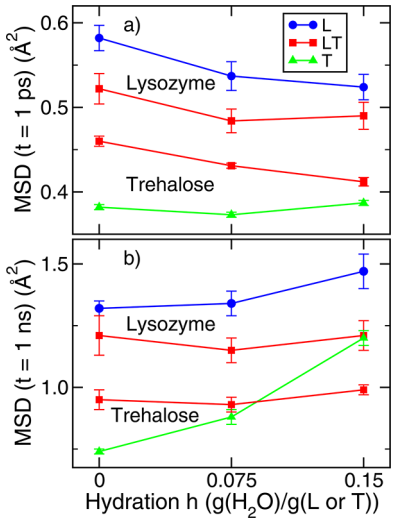

Figure 7. Mean square displacements (MSDs) of the hydrogens of lysozyme and trehalose in the different simulated systems as a function of the hydration level h: (a) at short time scale (t = 1 ps); (b) at long time scale (t = 1 ns).

Table 2. Mean Square Displacements (MSDs) of the Hydrogens of Water in the Different Hydrated Systems at Short (t = 1 ps) and Long (t = 1 ns) Time Scales[a]

	MSD(t = 1 ps) (Å^2)		MSD(t = 1 ns) (Å^2)	
system	h = 0.075	h = 0.15	h = 0.075	h = 0.15
L	0.97 (0.01)	1.05 (0.02)	26.5 (1.0)	60.1 (2.3)
LT	0.84 (0.01)	0.85 (0.01)	6.6 (0.1)	10.1 (0.2)
T	0.84 (0.01)	0.91 (0.01)	8.8 (0.1)	20.2 (0.6)

[a]Standard deviations from mean values are given in parentheses.

scale considered. Indeed, at the picosecond time scale, the MSD of lysozyme decreases upon addition of water, despite the larger MSD of the latter. This suggests an *antiplasticizing* effect of water in this concentration range on the protein fast motions, which can be accounted for by the significant increase of the number of hydrogen bonds formed by lysozyme that do not relax very much on this time scale (see next sections on HBs). This effect is fully consistent with the increased rigidity induced by low concentrations of water on amorphous sytems such as synthetic polymers[85] or food materials[86] at sub-T_g temperatures. It is particularly strong for the L glass, given the large holes that exist in the corresponding anhydrous glass (Figure 2), and it may explain why the apparent specific heat capacity of lysozyme was found slightly smaller at h = 0.07 than at h = 0.0 by Yang and Rupley.[87] In contrast, at the nanosecond time scale, the MSD of lysozyme increases with the water content, in agreement with previous neutron scattering experiments on lysozyme powders hydrated with D_2O, in which a systematic increase of $\langle u^2 \rangle$ with h was found in the 0.0−0.83 range.[88] This increase is also compatible with the activation of the slow relaxation of lysozyme observed at a slightly higher hydration level (h = 0.2), which was found to be correlated with its enzymatic activity.[89] Besides, the MSD of trehalose is found smaller than that of lysozyme, whatever the hydration level and time scale considered, in line with recent results on cytokine embedded in sucrose matrixes,[65] in which sucrose was found to decrease the amplitude of fast motions, thereby antiplasticizing the β-relaxation. However, the MSD of

dx.doi.org/10.1021/jp3058096 | J. Phys. Chem. B 2012, 116, 11103−11116

trehalose at the ns time scale increases much more with the water content than that of lysozyme. This clearly corroborates the well-known plasticizing effect of water on amorphous carbohydrate matrixes, that is, the strong decrease of their glass transition temperature, T_g, when the water content increases,[69,70] and it is in line with the diffusive motions of water occurring on this time scale (Table 2). Moreover, the MSD(t = 1 ps) of trehalose is smaller in the T matrix than in the LT one, in which most of the trehaloses are found in the vicinity of lysozymes. This result supports those from Dirama et al., which showed that the MSD of trehaloses at the surface of lysozyme are larger than that of bulk trehalose for temperatures below 450 K.[30] This effect can be explained by the more numerous and stronger T−T HBs formed in the T glass than in the LT one (see next sections on HBs). Finally, the MSD(t = 1 ns) values of lysozyme and trehalose do not change very much with the water content in the LT glass, implying that the added water molecules form a strong HB network with both lysozyme and trehalose, as proposed previously,[28] and consistent with the smaller MSDs of water found for the LT matrixes (Table 2). The MSDs of water are the largest in the L matrixes, since the filling by water of the large voids found in the anhydrous L glass (Figures 2 and 3) makes water−water interactions more likely (see Figure 8 and Table 3 in the next section) and leads to the formation of larger clusters of water (see Figures S1 and S2 in the Supporting Information). The strong reduction of the MSDs of water induced by trehalose is in line with its well-known retardation effect on the dynamics of water.[17,82,90−95] This effect may be ascribed to the formation of numerous trehalose−water HBs, which replace to a large extent the water−water HBs found in the hydrated L matrixes (see next section). It may also originate from the sterical hindering of the diffusion of water induced by the trehalose matrix. Note that the reduced mobility of water in the presence of trehalose may limit the chemical degradation of proteins that might occur during storage (deamidation, oxidation, etc.).[1]

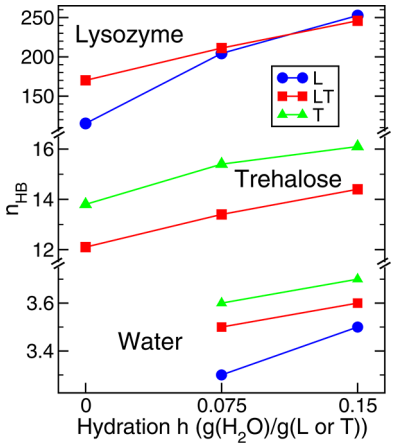

Figure 8. Total number of intermolecular HBs, n_{HB}, formed by lysozyme, trehalose, and water molecules in the different simulated systems as a function of the hydration level h. Standard deviations from mean values are smaller than the size of symbols and are thus not shown. Note that, for comparison, we previously found the n_{HB} of lysozyme in a dilute aqueous solution (h = 4.8) to be ∼330.[53] In addition, we obtained n_{HB} ∼ 18 and 4 for trehalose in a dilute aqueous solution (2 wt %) and for bulk water, respectively, using similar simulation conditions: force fields, HB geometric criterion, etc. (unpublished data).

Statistics of Hydrogen Bonds. The formation of numerous protein−sugar hydrogen bonds (HBs) is essential to explain why sugars such as trehalose and sucrose preserve proteins in freeze-dried matrixes.[1,2,4−9,11] Indeed, sugars may replace in the dry state the HBs formed by proteins in aqueous solutions and, thus, preserve their native structure and function (*water replacement* hypothesis[4,5]). In this study, we determined the intermolecular HBs formed between the different species following the same geometric criterion that we used previously for lysozyme in aqueous disaccharide solutions:[53] a hydrogen bond between a donor, D, and an acceptor, A, atom was considered to exist if the D···A distance was less than 3.4 Å and if the D−H···A angle was larger than 120°. Figure 8 shows the total number of intermolecular HBs, n_{HB}, that lysozyme, trehalose, and water form in the different systems, as a function of the hydration level h. The steep increase of the n_{HB} of lysozyme with h evidences that the full hydration of protein residues is not reached in the considered matrixes. Indeed, the n_{HB} of lysozyme was found close to 330 in an aqueous solution (h = 4.8).[53] These results are consistent with those from Joti et al. on hydrated staphylococcal nuclease, for which the total number of intermolecular HBs raises from 249.9 to 397.2 when h increases from 0.09 to 0.49.[96] The very low n_{HB} of lysozyme in the anhydrous L glass is ascribed in part to the large size of lysozyme, which limits its ability for intermolecular H-bonding with other protein neighbors, and it may explain why a severe dehydration might result in a change of the three-dimensional conformation of the protein.[97] At h = 0.0, the presence of trehalose significantly enhances the n_{HB} of lysozyme. Then, it becomes rather similar in the L and LT matrixes upon increasing h. These results imply that trehalose is able to replace the protein hydration water, as proposed previously,[5] but partially only, because of (i) the topological constraints imposed by its glucose rings on the relative positions of its hydroxyl groups and (ii) its much larger size in comparison with water, which prevents its close interaction with buried protein residues. Besides, as for lysozyme, the n_{HB} of trehalose is found lower in the anhydrous glass than in a dilute aqueous solution (∼18, unpublished data). The loss of about two HBs by trehalose in the presence of lysozyme is ascribed in part to excluded volume effects and suggests that lysozyme disorganizes the packing of trehalose, thus preventing an optimal protein−sugar H-bonding. This agrees with the lower density and the larger free volume fraction found for the LT glass with respect to the T one (see Figure 1). The loss of HBs by trehalose is also compatible with the positive excess enthalpy found for RNase A mixed with trehalose or sucrose at various sugar concentrations, which suggests that the new HBs formed in the mixture are either not as strong or not as numerous as those lost upon the disruption of self-interactions in the two pure components.[37] Finally, water molecules form less HBs in the considered matrixes than in the bulk (∼4), as expected from the presence of hydrophobic groups (CH, CH_2, CH_3), which limit the formation of protein−water (and protein−sugar) HBs. Interestingly, the n_{HB} of water in the different systems appear to be anticorrelated to the free volume fractions f (see Figure 1). This indicates that water molecules in the L and LT matrixes lose HBs when filling the buried clefts and cavities of lysozyme. In contrast, water molecules can hydrate trehalose with a smaller loss of HBs, given the large accessibility to water of the trehalose surface.

We then determined the contribution from each species to the n_{HB} to better understand the intermolecular H-bonding in

Table 3. Decomposition of the Mean Number of Intermolecular HBs, n_{HB}, Formed by Lysozyme, Trehalose, and Water Molecules in the Different Simulated Systems as a Function of the Hydration Level h

		lysozyme			trehalose			water		
system	h ($g_W/g_{L/T}$)	L−L	L−T	L−W	T−L	T−T	T−W	W−L	W−T	W−W
L	0.0	115.1								
	0.075	93.6		110.8				1.9		1.5
	0.15	79.6		173.0				1.5		2.1
LT	0.0	21.5	148.6		3.6	8.6				
	0.075	16.5	123.5	71.2	3.0	8.1	2.4	1.2	1.7	0.7
	0.15	19.9	106.7	119.4	2.6	7.7	4.2	1.0	1.5	1.1
T	0.0					13.8				
	0.075					11.6	3.8		2.7	1.0
	0.15					9.9	6.2		2.2	1.5

the studied matrixes (see Table 3). The addition of trehalose strongly reduces the number of protein−protein HBs, which are very few compared to L−T and L−W HBs in the LT glasses. This may partly explain why trehalose limits protein aggregation during storage, simply by physically separating proteins from each other.[98,99] In addition, the protein−water HBs represent about 37 and 53% of the intermolecular HBs formed by lysozyme with trehalose and water in the LT glasses at h = 0.075 and 0.15, respectively. Assuming that each water molecule may form 4 HBs and each hydroxyl group of trehalose 3, the expected proportions of protein−water HBs should be of 19.2 and 32.3%, respectively. The large excess of protein−water HBs compared to protein−trehalose HBs in the hydrated LT glasses indicates that lysozymes are preferentially hydrated, in agreement with the *preferential hydration* hypothesis[100] in dilute or semidilute solutions and with the *water entrapment* hypothesis[101] in the solid state. The *preferential* exclusion of osmolytes such as trehalose from the protein surface has indeed been shown to stabilize proteins in solution by making thermodynamically unfavorable the increase of their solvent accessible surface area (SASA) upon unfolding.[100] Belton and Gil have also hypothesized that, at low hydration, the protein hydration water is trapped by the solute glassy matrix, and that trehalose is able to concentrate the residual water in the vicinity of the protein.[101] We must still emphasize that, even though our results are consistent with the *preferential hydration* and with the *water entrapment* hypotheses, they do not explicitly show that trehalose stabilizes lysozyme. Indeed, on the time scale of our simulations (25 ns), no significant conformational change of lysozyme occurred in the L and LT matrixes (see Table S1 in the Supporting Information). As observed for lysozyme in aqueous sugar solutions,[53] the preferential hydration of lysozyme increases with the sugar weight fraction, and it corroborates the results from Cottone et al. for carboxy-myoglobin (MbCO) embedded in a 89 wt % trehalose/water matrix.[23,102] It can be ascribed to the size exclusion of trehalose from the surface cavities of lysozyme, as well as to the probably less favorable hydration of the hydroxyl groups of trehalose with respect to that of charged residues of lysozyme. Furthermore, in line with the preferential exclusion of trehalose from the surface of lysozyme, we found that 47 ± 2 and 34 ± 1% of the water molecules share HBs simultaneously with lysozyme and trehalose molecules in the hydrated LT glasses at hydration levels h of 0.075 and 0.15, respectively. The HBs that these bridging water molecules form with lysozyme account for 20 ± 1 and 16 ± 1%, respectively, of the total number of intermolecular HBs formed by lysozyme in these glasses, and 65 ± 2 and 60 ± 1% of them involve the ionic and polar groups of the side chains of lysozyme residues at hydration levels h of 0.075 and 0.15, respectively. These water molecules probably improve the protein−matrix dynamical coupling via the formation of a stiff water HB network at low water contents, as proposed by Cordone et al. (*water anchorage* hypothesis), who observed that the coupling of myoglobin to the embedding trehalose/water matrix becomes tighter when the water content decreases.[28] In addition, the number of trehalose−trehalose HBs, n_{HB}(T−T), overwhelms the number of lysozyme−trehalose HBs, n_{HB}(L−T), in the LT glasses, because of the large difference in size between lysozyme and trehalose, which makes T−T interactions sterically more likely. The large increase of the MSD of trehalose at the ns time scale in the T matrixes (Figure 7b) can be ascribed to the significant substitution of T−T HBs by T−W HBs, which represent almost 40% of the n_{HB} of trehalose at h = 0.15, and which relax much faster (Figure 10b). Finally, at a given hydration level h, water−water HBs are the most numerous in the hydrated L glasses, in which the significant excluded volume effects between lysozymes favor water−water interactions. The smaller size of trehalose compared to that of lysozyme as well as its high affinity for water[16,18] improve the homogeneity of the hydrated T and LT matrixes in comparison with the L ones, and thus reduce the probability for water−water interactions. This implies that water molecules are more confined and form smaller clusters (Figures S1 and S2 in the Supporting Information).

Geometry of Hydrogen Bonds. In the analysis performed above, we implicitly assumed that the different intermolecular HBs that satisfy the geometric criterion considered in this study are identical to each others. This is yet not true, given the heterogeneity of the groups involved in HBs (hydroxyls, carbonyls, carboxylates, etc.), and it implies that the different kinds of HBs are characterized by various geometries, strengths, and dynamics. In Figure 9, we show the length and angle distributions of various HBs formed in the L, T, and LT matrixes at h = 0.075. It immediately appears that the HBs that lysozyme and trehalose form with water are—on average—shorter and more linear, and thus stronger, than the ones they form with each other. This can be ascribed in part to the much stronger sterical and topological constraints that lysozyme and trehalose experience in comparison with water, which limit their abilities to interact as intimately with each other as water does. It may also originate from the lower dipole moments of the protein and sugar polar groups with respect to that of water. For example, in the carbohydrate[43,44] and water force fields used in this study,[45] the partial charges on the hydroxyl oxygen and hydrogen atoms of trehalose are equal to −0.65 e and

dx.doi.org/10.1021/jp3058096 | J. Phys. Chem. B 2012, 116, 11103−11116

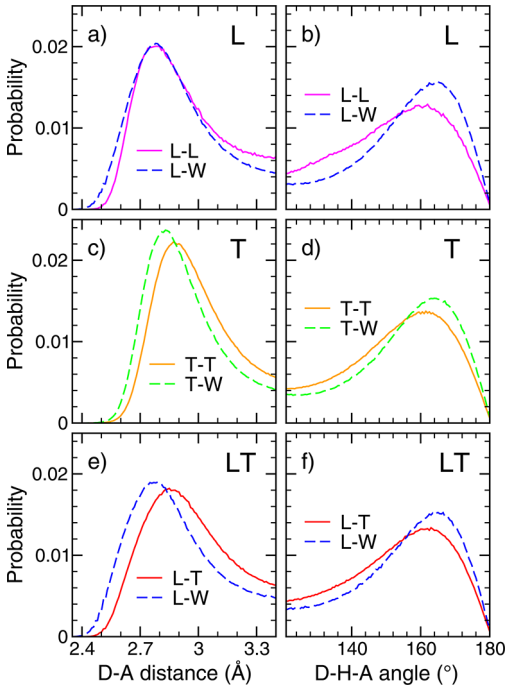

Figure 9. Distributions of the donor−acceptor distance (left) and donor−hydrogen−acceptor angle (right) of various HBs formed in the L (top), T (middle), and LT matrixes (bottom) at h = 0.075 (similar distributions are obtained at h = 0.0 and/or h = 0.15, and are thus not shown).

+0.41 e, respectively, whereas the oxygen and hydrogen atoms of water carry charges of −0.8476 e and +0.4238 e, respectively.

These results may explain the *antiplasticizing* effect of water on the vibrational and short-time motions of lysozyme and trehalose observed above (Figures 6 and 7), since the presence of water leads to an increase of both the number and the strength of the intermolecular HBs that lysozyme and trehalose form (Figures 8 and 9). At variance, the much larger mobility of water with respect to lysozyme and trehalose (Figure 7 and Table 2) is likely to make L−W and T−W HBs more labile than L−L, T−T, and L−T ones (see next section), thereby accounting for the *plasticizing* effect of water observed in Figure 7b and in other amorphous matrixes.[69,70] Besides, the more favorable interaction of lysozyme with water than with trehalose (Figure 9e,f) may explain why, beyond purely excluded volume effects, trehalose is *preferentially* excluded from the surface of proteins in the presence of water.[23,53,100]

Dynamics of Hydrogen Bonds. Finally, we have characterized the dynamics of HBs using the time autocorrelation function, $C_{HB}(t)$ defined as $C_{HB}(t) = \langle b(0)\cdot b(t)\rangle/\langle b\rangle$, where $b(t)$ is 1 if a D−H···A HB between a given set of donor, D, hydrogen, H, and acceptor, A, atoms exists at time t, and is zero otherwise.[103] The brackets mean averaging over the different pairs of HBs and time origins. By definition, $C_{HB}(t)$ relates to the probability that a HB formed at time 0 still exists at time t, even if it has broken in between. The short-time decay of $C_{HB}(t)$ stems from fast motions such as librations or intermolecular vibrations, and is therefore very sensitive to the strength of the HBs considered. In contrast, the long-time behavior of $C_{HB}(t)$ arises from the relative diffusion of the donor and acceptor atoms involved in the HBs and thus describes the structural relaxation of HBs.

Figure 10a and b clearly illustrates the *plasticizing effect* of water in the L and T amorphous matrixes. Indeed, at times

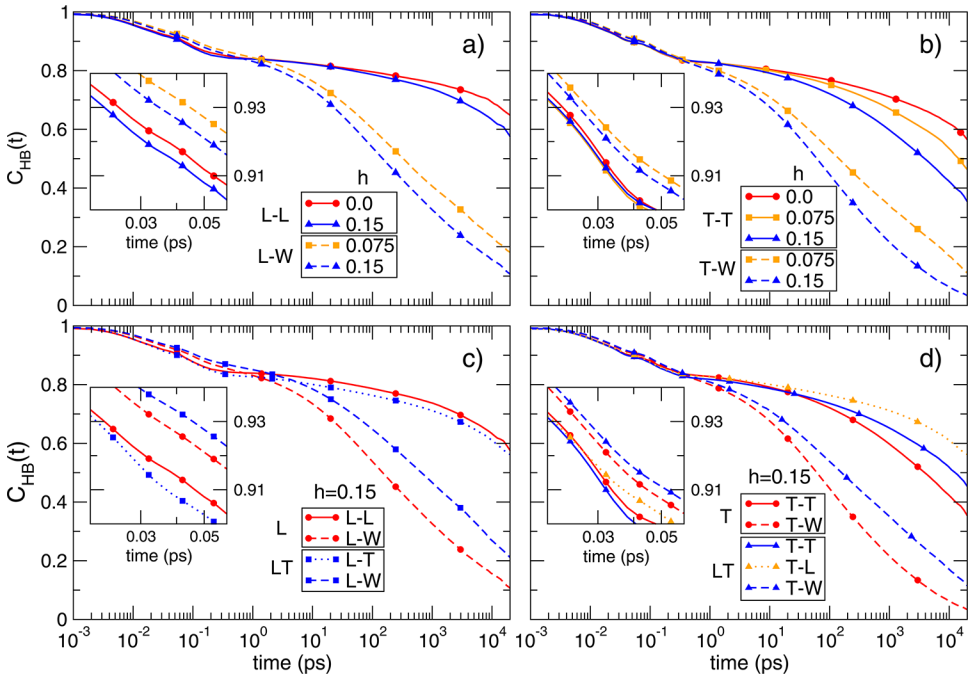

Figure 10. Time autocorrelation function C_{HB} of different types of HBs found in the studied matrixes. Top panel: The dependence on the hydration level h of the C_{HB} of the intermolecular HBs formed by lysozyme (L−L and L−W) and trehalose (T−T and T−W) in the L and T glasses is shown in parts a and b, respectively. Bottom panel: Comparison of the C_{HB} of the most abundant types of HBs formed by lysozyme (c) and trehalose (d) in the L and LT or T and LT matrixes. The insets show magnified views of the C_{HB} in the 0.02−0.06 ps range, where the decay is very sensitive to the strength of the HBs considered. Note that a correlation time of 0.055 ps corresponds to a frequency of about 600 cm^{-1}, that is, in the frequency range where the librational motions of water were observed in MD simulations of crystals and powders of RNase A.[104]

dx.doi.org/10.1021/jp3058096 | J. Phys. Chem. B 2012, 116, 11103−11116

larger than ∼10−100 ps, the C_{HB} of L−L and T−T HBs relax significantly faster in the presence of water. Moreover, the C_{HB} of L−W and T−W HBs decay much more rapidly than those of L−L and T−T HBs, respectively. Therefore, the structural relaxation of the intermolecular HBs that lysozyme and trehalose form in the hydrated L and T glasses, respectively, speeds up with the hydration level h. This accounts for the increase of MSD of lysozyme and trehalose when h increases (see Figure 7b). In addition, Figure 10c shows that at h = 0.15 L−L HBs in the L matrix relax slightly more slowly than L−T HBs in the LT glass. Thus, the decrease of the MSD of lysozyme induced by the presence of trehalose (Figure 7b) cannot be ascribed to the substitution of the L−L HBs found in the L matrix by the L−T HBs formed in the LT one (Table 3). Rather, it clearly appears that L−W HBs relax more slowly in the LT glass than in the L one. In other words, the relaxation of the protein hydration water is significantly slowed down in the presence of trehalose. This agrees with the well-known retardation effect of trehalose on the dynamics of water,[17,82,90−95] and it shows that the influence of trehalose on the dynamics of lysozyme is mediated by the protein hydration water. Moreover, Figure 10d shows that, at h = 0.15, both T−T and T−W HBs relax more slowly in the LT mixture. This is ascribed to the presence of lysozyme, which confines trehalose molecules and hinders its diffusion, as indicated by the slow relaxation of L−T HBs. This thus explains why the MSD of trehalose at t = 1 ns is much lower in the LT glass than in the T one at h = 0.15 (Figure 7). Interestingly, the short-time (<1 ps) behavior of C_{HB} might be opposite to that observed at longer times, where diffusive motions occur. The insets in Figure 10 show the C_{HB} in the 0.02−0.06 ps range, where the decay of C_{HB} primarily depends on the strength of the considered HBs. The intermolecular HBs that lysozyme and trehalose form with water appear stronger than the ones they formed with other lysozyme and/or trehalose molecules, in full agreement with their distance and angle distributions (Figure 9), which indicate that they are shorter and more linear. These results explain very well the reduction of the short-time MSDs of lysozyme and trehalose when h increases (Figure 7a). In particular, the inset of Figure 10c confirms that lysozyme−trehalose HBs are weaker than lysozyme−water ones (see also Figure 9e,f). The effect of trehalose on the vibrational and dynamical properties of lysozyme in the hydrated LT glasses is thus—partially at least—a consequence of the slowing down that trehalose induces on the structural relaxation of protein−water HBs.

DISCUSSION

Our results evidence that lysozyme is more rigid in the presence of trehalose. The number of low-frequency, anharmonic modes of lysozyme (Figure 6a) as well as the amplitude of its atomic motions (Figure 7a) are indeed significantly reduced in the LT glass compared to those in the L one. This is well in line with the lower quasi-elastic scattering intensity of lyophilized lysozyme/trehalose mixtures compared to that of hydrated lysozyme ($h \sim 0.35$) found by Caliskan et al. by means of Raman scattering experiments,[25] which indicates that trehalose reduces the protein flexibility. Previous neutron scattering and MD simulation studies[22,35] also showed that the amplitudes of the atomic motions of myoglobin are strongly reduced in the presence of trehalose in comparison with those in the presence of water. This may explain why trehalose stabilizes proteins against unfolding. Indeed, several studies clearly suggested an inverse relationship between the conformational flexibility of a protein and its thermal stability.[105−107] Similarly, the chemical and physical degradation rates of a series of proteins freeze-dried in the presence of trehalose or sucrose were shown to decrease with the mean square displacements of the matrixes.[34] In our simulations, the stiffening of lysozyme motions induced by trehalose appears correlated with the density increase and free volume decrease of the LT mixtures with respect to the L glasses (Figures 1−3). This result is fully consistent with the relationship between the free volume and the mean square displacement of model glass formers observed in previous MD simulation,[108] neutron scattering, and PALS[109] studies. By improving the molecular packing of the LT mixtures, trehalose significantly increases the number of intermolecular HBs formed by lysozyme in the dry state (Figure 8), which may improve its long-term stability. At variance with proteins in aqueous solutions, proteins in the dry state are surrounded by other proteins, which form HBs with each other that are stable on longer time scales than lysozyme−trehalose HBs (Figure 10c). Thus, in the dry state, the stabilization of proteins by trehalose probably stems not only from the substitution of protein−protein HBs by protein−trehalose HBs but also from the significant increase of the total number of intermolecular HBs formed by proteins (Figure 8). We further point out that trehalose could limit protein aggregation during storage by reducing drastically the number of protein−protein HBs (Table 3). It has actually been proposed that glass-forming excipients reduce protein aggregation in the solid state by "diluting" and physically separating proteins in the amorphous matrix.[98,99] Besides, trehalose replaces partially only the HBs formed by lysozyme in solution (Figure 8), since (i) it experiences a large sterical hindrance from the surface cavities of lysozyme as well as from small regions between neighboring lysozymes (Figure 4) and (ii) it interacts less favorably with lysozyme than water does (Figure 9e,f). Therefore, the replacement of all of the HBs formed by proteins in solution does not appear necessary for their long-term preservation in the dry state. Furthermore, the preferential exclusion of trehalose from the surface of lysozyme leaves space for water. As a consequence, water molecules are not homogeneously distributed in the hydrated LT glasses but are rather preferentially found in the vicinity of lysozyme, in accordance with the *preferential hydration*[100] and *water entrapment*[101] hypotheses. Note that this could explain why the addition of plasticizers—water, glycerol, sorbitol—at low concentrations may considerably improve the preservation of protein activity in disaccharide matrixes,[27,34,110] since these small additives could fit in the empty spaces at the protein−solvent interface from which the bigger disaccharides are size-excluded, and then improve the protein−matrix coupling. The preferential exclusion of trehalose from the surface of lysozyme implies that many waters form bridges between lysozyme and trehalose molecules (47 ± 2 and 34 ± 1% of the water molecules from the LT glass at hydration levels h of 0.075 and 0.15, respectively). These shared water molecules further increase the coupling between the vibrational motions of lysozyme and trehalose, in agreement with the *anchorage* hypothesis proposed by Cordone et al.[28] However, it must be emphasized that the number of lysozyme−trehalose HBs is significantly larger than that of lysozyme−water HBs in the LT glass at h = 0.075 (∼124 vs ∼71, see Table 3). This means that the interactions between lysozyme and trehalose remain essentially mediated by direct hydrogen bonding between

them at low water contents, as observed by Allison et al. for different freeze-dried lysozyme/sugar matrixes by Fourier transform infrared spectroscopy.[6] Besides, lysozyme forms a similar total number of intermolecular HBs in the L and LT matrixes at hydration levels h of 0.075 and 0.15 (Figure 8). Thus, the stiffening of the vibrational motions of lysozyme in the LT glass cannot be explained by a larger number of HBs formed by lysozyme in the presence of trehalose. One could then expect that lysozyme is less flexible in the LT glass, because it forms with trehalose HBs that are *stronger* than the ones it makes with water in the L matrixes. However, the time correlation function C_{HB} of lysozyme−trehalose HBs actually decays faster than the C_{HB} of lysozyme−water HBs at subpicosecond time scales (Figure 10c), therefore indicating that L−T HBs are *weaker* than L−W ones in our simulations. This is confirmed by the longer and more bent HBs that trehalose form with lysozyme compared to the protein−water HBs (Figure 9e,f). We ascribe the lower strength of the L−T HBs to the lower dipole moment of the sugar hydroxyl groups compared to that of water, as well as to the larger sterical hindrance that trehalose experiences, which imposes severe constraints on the geometry of the protein−sugar HBs. Nevertheless, L−T HBs relax much more slowly at long time scales (∼ns) than L−W HBs (Figure 10c), given the much lower mobility of trehalose (Figure 7 and Table 2), which is much heavier (mass of 342.3 g·mol^{-1}) than water. The stiffening of the motions of lysozyme in the presence of trehalose in the hydrated LT matrixes appears to partly arise from the slowing down of the relaxation of lysozyme−water HBs induced by trehalose (Figure 10c), which is likely to result from the one it induces on water dynamics.[17,82,90−95] Actually, it was shown previously that the structural relaxation time of water and the water−water HB lifetime in trehalose aqueous solutions strongly increase with the sugar concentration.[82,91] Both the translational and rotational motions of water were found slowed down in the vicinity of trehalose,[92,95] and the relaxation time of water−water HBs was found larger than that of bulk water up to a distance of ∼6.5 Å from the trehalose surface.[93] The slowing down of water dynamics was ascribed to the formation of stable carbohydrate−water HBs[92] and also, in part, to excluded volume effects that make the exchange of water−water HBs less likely in the vicinity of trehalose than in bulk water.[95] Such a solute excluded volume effect does not require the formation of water−solute HBs, and it was shown to explain the rotational slowing down of water near the hydrophobic methyl groups of trimethylamine-*N*-oxide (TMAO).[111] It may partly explain why in our simulations trehalose slows down the dynamics of water without forming very strong HBs with it. Indeed, trehalose forms at high concentrations a matrix that is stiffened by a percolating network of trehalose−trehalose HBs,[112,113] which relax much more slowly than T−W and L−W HBs (Figure 10). This stiff matrix sterically hinders the exchange of HBs between water molecules and then makes water less mobile in the hydrated LT matrixes than in the L ones (Table 2). Given the well-known correlation between the mobility of the solvent and protein fluctuations,[114] trehalose thereby reduces the probability of large-scale motions of proteins that may lead to their degradation.[34]

CONCLUSION

Our comparative study of the lysozyme (L), lysozyme/trehalose (LT), and trehalose (T) matrixes has provided valuable information on the protein−matrix interactions at low hydration levels, which may help in deciphering the stabilizing effect of trehalose on proteins during storage. The presence of trehalose significantly improves the molecular packing of lysozyme, so that the large voids found in the dry L glass vanish in the dry LT mixture. A strong protein−matrix coupling is evidenced in the LT system from the mutual influence of lysozyme and trehalose on the vibrational and dynamical properties of each other. Trehalose appears to make lysozyme more rigid, as observed previously,[22,25,35] and thus less likely to unfold, given the inverse relationship between protein flexibility and stability.[105−107] Our results also emphasize the peculiar role played by water in these matrixes. Indeed, at low concentration (h = 0.075), water reduces the amplitude of the vibrational motions of lysozyme and trehalose, thereby suggesting that it acts as an *antiplasticizer* on their fast motions. In contrast, water increases the MSDs of lysozyme and trehalose on the ns time scale, in good agreement with its well-known *plasticizing* effect on amorphous matrixes.[69,70] The influence of trehalose and water on lysozyme is fully accounted for by our analysis of the intermolecular HBs formed in these matrixes. In the dry state, the decrease of the flexibility of lysozyme induced by trehalose obviously stems from the significant increase of the number of intermolecular HBs formed by lysozyme. Trehalose indeed intercalates between neighboring proteins and forms numerous HBs with them. However, it is not able to replace all the HBs formed by lysozyme with water in aqueous solution, since its larger size and more complex topology do not allow it to interact with proteins as intimately as water does. Accordingly, lysozyme interacts *preferentially*[100] with water in the hydrated LT matrixes, as observed previously for myoglobin in concentrated trehalose matrixes.[23] Furthermore, trehalose slows down the structural relaxation of lysozyme−water HBs, in accordance with its well-known retardation effect on the dynamics of water in solution.[17,82,90−95] This effect mainly originates from the numerous HBs that it makes with water as well as from the stiff matrix it forms, which sterically hinders the diffusion of water. Moreover, the lysozyme−water HBs are found shorter and more linear, and thus *stronger*, than the lysozyme−trehalose ones. However, their structural relaxation is faster at the ns time scale, given the larger mobility of water compared to that of trehalose. Therefore, in hydrated matrixes, part of the stabilizing effect of trehalose on proteins probably arises from its ability to limit the long-time structural relaxation of the HBs that proteins form with water.

ASSOCIATED CONTENT

Supporting Information

Average contents of α-helices and β-sheets of lysozyme in the L and LT matrixes, spatial distributions of water clusters in the matrixes at h = 0.075, and size distributions of water clusters. This material is available free of charge via the Internet at http://pubs.acs.org.

AUTHOR INFORMATION

Corresponding Author

*E-mail: adrien.lerbret@u-bourgogne.fr.

Present Address

⊥AgroSup Dijon, 1 Esplanade Erasme, 21000 Dijon, France.

Notes

The authors declare no competing financial interest.

■ ACKNOWLEDGMENTS

This work was supported by the "INTERREG IVA 2 Mers Seas Zeeën Cross-border Cooperation Programme 2007-2013" and by the ANR (Agence Nationale de la Recherche) through the BIOSTAB project ("Physique-Chimie du Vivant" program). It was granted access to the HPC resources of IDRIS under the allocation 2010-0629 made by the GENCI (Grand Equipement National de Cacul Intensif). A.L. thanks the Nord-Pas de Calais region for a postdoctoral fellowship. Dr. Stéphane Longeville from Laboratoire Léon Brillouin (CEA-Saclay, France) is acknowledged for his assistance during the neutron scattering experiments.

■ REFERENCES

(1) Wang, W. *Int. J. Pharm.* **2000**, *203*, 1−60.
(2) Hill, J. J.; Shalaev, E. Y.; Zografi, G. *J. Pharm. Sci.* **2005**, *94*, 1636−1667.
(3) Green, J. L.; Angell, C. A. *J. Phys. Chem.* **1989**, *93*, 2880−2882.
(4) Crowe, J. H.; Crowe, L. M.; Chapman, D. *Science* **1984**, *223*, 701−703.
(5) Crowe, J. H.; Carpenter, J. F.; Crowe, L. M. *Annu. Rev. Physiol.* **1998**, *60*, 73−103.
(6) Allison, S. D.; Chang, B.; Randolph, T. W.; Carpenter, J. F. *Arch. Biochem. Biophys.* **1999**, *365*, 289−298.
(7) López-Diez, E. C.; Bone, S. *Biochim. Biophys. Acta* **2004**, *1673*, 139−148.
(8) Chang, L.; Sheperd, D.; Sun, J.; Ouellette, D.; Grant, K. L.; Tang, X.; Pikal, M. J. *J. Pharm. Sci.* **2005**, *94*, 1427−1444.
(9) Sakurai, M.; Furuki, T.; Akao, K.-I.; Tanaka, D.; Nakahara, Y.; Kikawada, T.; Watanabe, M.; Okuda, T. *Proc. Natl. Acad. Sci. U.S.A.* **2008**, *105*, 5093−5098.
(10) Gottfried, D. S.; Peterson, E. S.; Sheikh, A. G.; Wang, J.; Yang, M.; Friedman, J. M. *J. Phys. Chem.* **1996**, *100*, 12034−12042.
(11) Carpenter, J. F.; Crowe, J. H. *Biochemistry* **1989**, *28*, 3916−3922.
(12) Jain, N. K.; Roy, I. *Protein Sci.* **2009**, *18*, 24−36.
(13) Yancey, P. H. *J. Exp. Biol.* **2005**, *208*, 2819−2830.
(14) Miller, D. P.; de Pablo, J. J.; Corti, H. *Pharm. Res.* **1997**, *14*, 578−590.
(15) Sussich, F.; Skopec, C.; Brady, J.; Cesàro, A. *Carbohydr. Res.* **2001**, *334*, 165−176.
(16) Branca, C.; Magazù, S.; Maisano, G.; Migliardo, F.; Migliardo, P.; Romeo, G. *J. Phys. Chem. B* **2001**, *105*, 10140−10145.
(17) Magazù, S.; Villari, V.; Migliardo, P.; Maisano, G.; Telling, M. T. F. *J. Phys. Chem. B* **2001**, *105*, 1851−1855.
(18) Furuki, T.; Oku, K.; Sakurai, M. *Front. Biosci.* **2009**, *14*, 3523−3535.
(19) Miller, D. P.; de Pablo, J. J. *J. Phys. Chem. B* **2000**, *104*, 8876−8883.
(20) Taga, T.; Senma, M.; Osaki, K. *Acta Crystallogr.* **1972**, *B28*, 3258−3263.
(21) Aldous, B. J.; Auffret, A. D.; Franks, F. *CryoLetters* **1995**, *16*, 181−186.
(22) Cottone, G.; Cordone, L.; Ciccotti, G. *Biophys. J.* **2001**, *80*, 931−938.
(23) Cottone, G.; Ciccotti, G.; Cordone, L. *J. Chem. Phys.* **2002**, *117*, 9862−9866.
(24) Giuffrida, S.; Cottone, G.; Librizzi, F.; Cordone, L. *J. Phys. Chem. B* **2003**, *107*, 13211−13217.
(25) Caliskan, G.; Kisliuk, A.; Tsai, A. M.; Soles, C. L.; Sokolov, A. P. *J. Chem. Phys.* **2003**, *118*, 4230−4236.
(26) Caliskan, G.; Mechtani, D.; Roh, J. H.; Kisliuk, A.; Sokolov, A. P.; Azzam, S.; Cicerone, M. T.; Lin-Gibson, S.; Peral, I. *J. Chem. Phys.* **2004**, *121*, 1978−1983.
(27) Cicerone, M. T.; Soles, C. L. *Biophys. J.* **2004**, *86*, 3836−3845.
(28) Cordone, L.; Cottone, G.; Giuffrida, S.; Palazzo, G.; Venturoli, G.; Viappiani, C. *Biochim. Biophys. Acta* **2005**, *1749*, 252−281.
(29) Massari, A. M.; Finkelstein, I. J.; McClain, B. L.; Goj, A.; Wen, X.; Bren, K. L.; Loring, R. F.; Fayer, M. D. *J. Am. Chem. Soc.* **2005**, *127*, 14279−14289.
(30) Dirama, T. E.; Curtis, J. E.; Carri, G. A.; Sokolov, A. P. *J. Chem. Phys.* **2006**, *124*, 034901.
(31) Curtis, J. E.; Dirama, T. E.; Carri, G. A.; Tobias, D. J. *J. Phys. Chem. B* **2006**, *110*, 22953−22956.
(32) Bellavia, G.; Cottone, G.; Giuffrida, S.; Cupane, A.; Cordone, L. *J. Phys. Chem. B* **2009**, *113*, 11543−11549.
(33) Bellavia, G.; Giuffrida, S.; Cottone, G.; Cupane, A.; Cordone, L. *J. Phys. Chem. B* **2011**, *115*, 6340−6346.
(34) Cicerone, M. T.; Douglas, J. F. *Soft Matter* **2012**, *8*, 2983−2991.
(35) Cordone, L.; Ferrand, M.; Vitrano, E.; Zaccai, G. *Biophys. J.* **1999**, *76*, 1043−1047.
(36) Kawai, K.; Suzuki, T. *Pharm. Res.* **2007**, *24*, 1883−1890.
(37) Katayama, D. S.; Carpenter, J. F.; Menard, K. P.; Manning, M. C.; Randolph, T. W. *J. Pharm. Sci.* **2009**, *98*, 2954−2969.
(38) Rupley, J. A.; Careri, G. *Adv. Protein Chem.* **1991**, *41*, 37−172.
(39) Brooks, B. R.; Bruccoleri, R. E.; Olafson, B. D.; States, D. J.; Swaminathan, S.; Karplus, M. *J. Comput. Chem.* **1983**, *4*, 187−217.
(40) Brooks, B. R.; et al. *J. Comput. Chem.* **2009**, *30*, 1545−1614.
(41) MacKerell, A. D.; et al. *J. Phys. Chem. B* **1998**, *102*, 3586−3616.
(42) MacKerell, A. D.; Feig, M.; Brooks, C. L. *J. Comput. Chem.* **2004**, *25*, 1400−1415.
(43) Guvench, O.; Greene, S. N.; Kamath, G.; Brady, J. W.; Venable, R. M.; Pastor, R. W.; MacKerell, A. D. *J. Comput. Chem.* **2008**, *29*, 2543−2564.
(44) Guvench, O.; Hatcher, E.; Venable, R. M.; Pastor, R. W.; MacKerell, A. D. *J. Chem. Theory Comput.* **2009**, *5*, 2353−2370.
(45) Berendsen, H. J. C.; Grigera, J. R.; Straatsma, T. P. *J. Phys. Chem.* **1987**, *91*, 6269−6271.
(46) Ryckaert, J. P.; Ciccotti, G.; Berendsen, H. J. C. *J. Comput. Phys.* **1977**, *23*, 327−341.
(47) Hockney, R. W. *Methods Comput. Phys.* **1970**, *9*, 135−211.
(48) Steinbach, P. J.; Brooks, B. R. *J. Comput. Chem.* **1994**, *15*, 667−683.
(49) Essmann, U.; Perera, L.; Berkowitz, M. L.; Darden, T.; Lee, H.; Pedersen, L. G. *J. Chem. Phys.* **1995**, *103*, 8577−8593.
(50) Nosé, S.; Klein, M. L. *J. Chem. Phys.* **1983**, *78*, 6928−6939.
(51) Hoover, W. G. *Phys. Rev. A* **1985**, *31*, 1695−1697.
(52) Sterpone, F.; Ceccarelli, M.; Marchi, M. *J. Mol. Biol.* **2001**, *311*, 409−419.
(53) Lerbret, A.; Bordat, P.; Affouard, F.; Hédoux, A.; Guinet, Y.; Descamps, M. *J. Phys. Chem. B* **2007**, *111*, 9410−9420.
(54) Oleinikova, A.; Smolin, N.; Brovchenko, I. *Biophys. J.* **2007**, *93*, 2986−3000.
(55) Vaney, M. C.; Maignan, S.; Riès-Kautt, M.; Ducruix, A. *Acta Crystallogr., Sect. D* **1996**, *52*, 505−517.
(56) Dirama, T. E.; Carri, G. A.; Sokolov, A. P. *J. Chem. Phys.* **2005**, *122*, 114505.
(57) Riggleman, R. A.; de Pablo, J. J. *J. Chem. Phys.* **2008**, *128*, 224504.
(58) Magazù, S.; Migliardo, F.; Affouard, F.; Descamps, M.; Telling, M. T. F. *J. Chem. Phys.* **2010**, *132*, 184512.
(59) Imamura, K.; Maruyama, Y.; Tanaka, K.; Yokoyama, T.; Imanaka, H.; Nakanishi, K. *J. Pharm. Sci.* **2008**, *97*, 2789−2797.
(60) Zhang, J.; Zografi, G. *J. Pharm. Sci.* **2001**, *90*, 1375−1385.
(61) Kikuchi, T.; Wang, B.; Pikal, M. J. *J. Pharm. Sci.* **2011**, *100*, 2945−2951.
(62) Kundrot, C. E.; Richards, F. M. *J. Mol. Biol.* **1988**, *200*, 401−410.
(63) White, E. T.; Tan, W. H.; Ang, J. M.; Tait, S.; Litster, J. D. *Powder Technol.* **2007**, *179*, 55−58.
(64) Gabel, F.; Bicout, D.; Lehnert, U.; Tehei, M.; Weik, M.; Zaccai, G. *Q. Rev. Biophys.* **2002**, *35*, 327−367.
(65) Wang, B.; Tchessalov, S.; Cicerone, M. T.; Warne, N. W.; Pikal, M. J. *J. Pharm. Sci.* **2009**, *98*, 3145−3166.
(66) Townrow, S.; Roussenova, M.; Giardiello, M.-I.; Alam, A.; Ubbink, J. *J. Phys. Chem. B* **2010**, *114*, 1568−1578.

(67) Roussenova, M.; Murith, M.; Alam, A.; Ubbink, J. *Biomacromolecules* **2010**, *11*, 3237−3247.
(68) Simperler, A.; Kornherr, A.; Chopra, R.; Jones, W.; Motherwell, W. D. S.; Zifferer, G. *Carbohydr. Res.* **2007**, *342*, 1470−1479.
(69) Roos, Y. *Carbohydr. Res.* **1993**, *238*, 39−48.
(70) Hancock, B. C.; Zografi, G. *Pharm. Res.* **1994**, *11*, 471−477.
(71) Limbach, H. J.; Ubbink, J. *Soft Matter* **2008**, *4*, 1887−1898.
(72) Molinero, V.; Çağin, T.; Goddard, W. A., III. *Chem. Phys. Lett.* **2003**, *377*, 469−474.
(73) Humphrey, W.; Dalke, A.; Schulten, K. *J. Mol. Graphics* **1996**, *14*, 33−38.
(74) Balog, E.; Becker, T.; Oettl, M.; Lechner, R.; Daniel, R.; Finney, J.; Smith, J. C. *Phys. Rev. Lett.* **2004**, *93*, 028103.
(75) Balog, E.; Perahia, D.; Smith, J. C.; Merzel, F. *J. Phys. Chem. B* **2011**, *115*, 6811−6817.
(76) Lerbret, A.; Affouard, F.; Bordat, P.; Hédoux, A.; Guinet, Y.; Descamps, M. *J. Chem. Phys.* **2009**, *131*, 245103.
(77) Balog, E.; Smith, J. C.; Perahia, D. *Phys. Chem. Chem. Phys.* **2006**, *8*, 5543−5548.
(78) Doster, W. *Biochim. Biophys. Acta* **2010**, *1804*, 3−14.
(79) Idrissi, A.; Longelin, S.; Sokolic, F. *J. Phys. Chem. B* **2001**, *105*, 6004−6009.
(80) Padro, J. A.; Marti, J. *J. Chem. Phys.* **2003**, *118*, 452−453.
(81) Savitzky, A.; Golay, M. J. E. *Anal. Chem.* **1964**, *36*, 1627−1639.
(82) Lerbret, A.; Affouard, F.; Bordat, P.; Hédoux, A.; Guinet, Y.; Descamps, M. *J. Non-Cryst. Solids* **2011**, *357*, 695−699.
(83) Chakraborty, S.; Sinha, S. K.; Bandyopadhyay, S. *J. Phys. Chem. B* **2007**, *111*, 13626−13631.
(84) Heyden, M.; Havenith, M. *Methods* **2010**, *52*, 74−83.
(85) Dlubek, G.; Redmann, F.; Krause-Rehberg, R. *J. Appl. Polym. Sci.* **2002**, *84*, 244−255.
(86) Seow, C. C.; Cheah, P. B.; Chang, Y. P. *J. Food Sci.* **1999**, *64*, 576−581.
(87) Yang, P.-H.; Rupley, J. A. *Biochemistry* **1979**, *18*, 2654−2661.
(88) Paciaroni, A.; Cinelli, S.; Onori, G. *Biophys. J.* **2002**, *83*, 1157−1164.
(89) Roh, J. H.; Curtis, J. E.; Azzam, S.; Novikov, V. N.; Peral, I.; Chowdhuri, Z.; Gregory, R. B.; Sokolov, A. P. *Biophys. J.* **2006**, *91*, 2573−2588.
(90) Rampp, M.; Buttersack, C.; Ludemann, H. D. *Carbohydr. Res.* **2000**, *328*, 561−572.
(91) Bordat, P.; Lerbret, A.; Demaret, J.-P.; Affouard, F.; Descamps, M. *Europhys. Lett.* **2004**, *65*, 41−47.
(92) Lee, S. L.; Debenedetti, P. G.; Errington, J. R. *J. Chem. Phys.* **2005**, *122*, 204511.
(93) Heyden, M.; Brundermann, E.; Heugen, U.; Niehues, G.; Leitner, D. M.; Havenith, M. *J. Am. Chem. Soc.* **2008**, *130*, 5773−5779.
(94) Paolantoni, M.; Comez, L.; Gallina, M. E.; Sassi, P.; Scarponi, F.; Fioretto, D.; Morresi, A. *J. Phys. Chem. B* **2009**, *113*, 7874−7878.
(95) Vila Verde, A.; Campen, R. K. *J. Phys. Chem. B* **2011**, *115*, 7069−7084.
(96) Joti, Y.; Nakagawa, H.; Kataoka, M.; Kitao, A. *J. Phys. Chem. B* **2008**, *112*, 3522−3528.
(97) Costantino, H. R.; Griebenow, K.; Mishra, P.; Langer, R.; Klibanov, A. M. *Biochim. Biophys. Acta* **1995**, *1253*, 69−74.
(98) Wang, W. *Int. J. Pharm.* **2005**, *289*, 1−30.
(99) Perez-Moral, N.; Adnet, C.; Noel, T. R.; Parker, R. *Biomacromolecules* **2010**, *11*, 2985−2992.
(100) Timasheff, S. N. *Biochemistry* **2002**, *41*, 13473−13482.
(101) Belton, P. S.; Gil, A. M. *Biopolymers* **1994**, *34*, 957−961.
(102) Cottone, G.; Giuffrida, S.; Ciccotti, G.; Cordone, L. *Proteins: Struct., Funct., Bioinform.* **2005**, *59*, 291−302.
(103) Luzar, A.; Chandler, D. *Phys. Rev. Lett.* **1996**, *76*, 928−931.
(104) Tarek, M.; Tobias, D. J. *Biophys. J.* **2000**, *79*, 3244−3257.
(105) Tang, K. E. S.; Dill, K. A. *J. Biomol. Struct. Dyn.* **1998**, *16*, 397−411.
(106) Tsai, A. M.; Udovic, T. J.; Neumann, D. A. *Biophys. J.* **2001**, *81*, 2339−2343.
(107) Cornicchi, E.; Marconi, M.; Onori, G.; Paciaroni, A. *Biophys. J.* **2006**, *91*, 289−297.
(108) Starr, F. W.; Sastry, S.; Douglas, J. F.; Glotzer, S. C. *Phys. Rev. Lett.* **2002**, *89*, 125501.
(109) Ottochian, A.; Leporini, D. *J. Non-Cryst. Solids* **2011**, *357*, 298−301.
(110) Chang, L.; Sheperd, D.; Sun, J.; Tang, X.; Pikal, M. J. *J. Pharm. Sci.* **2005**, *94*, 1445−1455.
(111) Laage, D.; Stirnemann, G.; Hynes, J. T. *J. Phys. Chem. B* **2009**, *113*, 2428−2435.
(112) Lerbret, A.; Bordat, P.; Affouard, F.; Descamps, M.; Migliardo, F. *J. Phys. Chem. B* **2005**, *109*, 11046−11057.
(113) Sapir, L.; Harries, D. *J. Phys. Chem. B* **2011**, *115*, 624−634.
(114) Vitkup, D.; Ringe, D.; Petsko, G. A.; Karplus, M. *Nat. Struct. Biol.* **2000**, *7*, 34−38.